Multi-Objective Optimisation-based Robust H∞ Controller Design Approach for a Multi-Level DC-DC Voltage Regulator

Ridvan Keskin[1, *], Ibrahim Aliskan[2]
[1]*Department of Electrical and Electronics Engineering, Zonguldak Bulent Ecevit University, Zonguldak, Turkey*
[2]*Department of Control and Automation Engineering, Yildiz Technical University, Istanbul, Turkey*
[*]*ridvan.keskin@beun.edu.tr, aliskan@yildiz.edu.tr*

***Abstract*—In case an analytical approach to the selection of any weighting function is not possible, the selection process is usually a random and time-consuming process. In robust H∞ control theory, the selection of scalar, time, or frequency-dependent weighting functions is the main issue to shape the amplitude-frequency characteristic curve of the feedback controller. Therefore, we propose a robust H∞ control approach which utilises the multi-objective grey wolf optimisation algorithm (MOGWO) to obtain the optimal performance weighting functions in the presence of right half-plane zeros and limited bandwidth constraints. A trade-off design flowchart is proposed, providing Pareto optimal solutions to choose the optimal configuration of the robust feedback controller. The control method is structured by combining the robust H∞ optimal technique and the multi-objective algorithm. The effectiveness of the approach is compared with the non-convex single-objective heuristic solutions like the multi-verse optimisation algorithm (MVO), whale optimisation algorithm (WOA), and grey wolf optimisation algorithm (GWO). The focus of this design is to track and stabilise the output voltage of the DC-DC converter in the presence of external disturbances and parameter uncertainties. The optimised controllers are implemented using a digital signal processor (DSP) on a 200 W interleaved boost converter. The simulation results and experimental findings show that the proposed control method provides supreme disturbance rejection along with maintaining the stability of the system.**

***Index Terms*—Meta-heuristic optimisation; Multi-objective optimisation; Robust control; DC-DC converter.**

I. INTRODUCTION

Multi-phase DC-DC converters are widely preferred to fix the source terminal voltage to a higher value in any renewable energy resources or power transmission lines of electric vehicles [1], [2]. The converters keep the output voltage at a certain value in case of input voltage and load current variations of the converter [3], [4]. The output voltage stability of the battery or fuel cell stack with a DC-DC converter presents a fundamental challenge to the reliability of any DC-link lines and power transmission lines of any electric vehicle, since uncertainties, sensor noise, load, and input voltage disturbances cause system instability [5], [6]. Robust H∞ control-based controllers provide robust performance and stability in addition to minimising the effects of the mentioned problems on the control system. In robust H∞ control theory, loop shaping control techniques enable reliable robust performance with the right choice of weighting functions, which is influenced by several variables, including roll-off rates, bandwidth, and low-frequency gain. The choice of reference, output performance, and disturbance weighting functions in the H∞ robust control optimisation procedure straightforwardly characterise the robustness of the system and transient performance requirements [7]. The choice which is usually based on the experience of the designer or the trial-error process results in a time-consuming process [8]–[11]. Some researchers attempted to establish a quantitative relationship between the performance of the control system and the output performance weighting functions using an analytical approach [12]. However, the quantitative relationship is so complex that it is nearly impossible to determine the relationship. Other researchers point out the engineering experience for the design of weighting functions in the H∞ control.

Recently, meta-heuristic algorithms gained significant interest and demonstrated promising results in the multi-dimensional parameter optimisation of all types of non-convex or non-smooth optimisation problems [13], [14]. Genetic algorithm (GA) [15], particle swarm optimisation algorithm (PSO) [16], gravitational search algorithm [17], grey wolf optimisation algorithm (GWO) [18], whale optimisation algorithm (WOA) [19], multi-verse optimisation algorithm (MVO) [20], and multi-objective grey wolf optimisation algorithm (MOGWO) [21] are highly preferred to find the optimum design parameters of any non-convex problems. A PSO-based approach is proposed to optimise the weighting matrices of the optimal full-state controller (LQR) [22], [23]. A single-objective hybrid algorithm-based active disturbance rejection controller tuning method is proposed to improve the transient response of the control system [24]. A robust adaptive fuzzy control that utilises the GA algorithm is proposed to find the parameters of the fuzzy structure under external disturbances [25]. The algorithm is combined with a non-

Manuscript received 30 November, 2022; accepted 18 January, 2023.

linear model predictive controller process to obtain the exact model of a non-linear system [26]. The authors in [27] propose an automatic loop shaping method with GAs. The weighting functions of the aforementioned control approaches consist of only scalar values. The design of controllers in this case is a simple problem.

The GA is used to tune the weighting functions of the H∞ K-Glover and McFarlane method. However, it has disadvantages such as convergence speed and low exploration. The authors in [28] propose a robust structured GA-based H∞ control process. Adaptive mutation-based PSO (AMBPSO) is proposed for multi-variable robust H∞ control design [29]. These approaches with a single-objective function only optimise parameters depending on the error signal of the measured variable. A H_2–H∞ robust control method is proposed to optimise the weights of the method using the hybrid particle swarm optimisation and the gravitational search algorithm [30]. A chaos optimisation algorithm-based robust H∞ control design with mixed sensitivity approach is proposed for a piezoelectric actuator system [31]. The objective function of the process, however, considers only time-domain metrics, i.e., the reference signal tracking error and maximum overshoot values. The authors in [32] propose a robust PSO-based controller design. The process considers only the minimisation of the $\|.\|_\infty$ norm of the controlled system. In this case, although the stability of the system is increased, the system loses performance under the reference changes and disturbance effects. In objective functions created by combining more than one objective function, the weighting factors depend on the designer. Although the objective function is multivariate, it does not serve multiple purposes. A robust H∞ loop-shaping controller design procedure based on multi-objective genetic algorithm (MOGA) is proposed in [33]. The algorithm is combined with the classic K-Glover and McFarlane methods. However, this approach does not consider parameter uncertainty and disturbance effects. Another MOGA-based robust H∞ control design combined with a mixed sensitivity approach is proposed in [34]. The objective function employs the maximum overshoot, settling time, steady-state error, and the inductance current upper bound. A robust multi-objective method that considers stability and performance criteria would be the solution to the mentioned problems.

In robust H∞ control theory, the selection of frequency-dependent weighting functions is the main problem for obtaining a strong feedback controller, which is a time-consuming process and there is no analytical method to solve this problem. The novelty of the paper is that the control method is constructed by combining the robust H∞ optimal technique and the multi-objective algorithm. In addition, the objective function of the algorithm is structured as an infinite norm of performance weights and an integral squared error of the measured variable. The work focuses on applying robust H∞ control theory to improve the transient response and disturbance rejection performance of the converter and combines the MOGWO and the two-Riccati approach to optimise weighting functions for control input, measured variable, and error performance. The contributions of this work are as follows:

– A robust H_∞ multi-objective approach is proposed to optimise the performance weighting functions;

– The H_∞ performance weighting functions based on the frequency domain are optimised with the proposed multi-objective approach and compared with the single-objective heuristic algorithms;

– The multi-objective optimisation problem is structured with the reference voltage tracking error and infinite norm $\|.\|_\infty$ metrics;

– The controllers are implemented on a two-phase interleaved boost converter (IBC).

The paper is structured as follows. In Section II, the single- and multi-objective algorithms are described. Section III presents the noise, control-to-output models of the converter, and the proposed robust H∞ controller design steps. Section IV presents simulation results and results from real-time applications based on the digital signal processor (DSP). Section V discusses the results of the works.

II. Optimisation Algorithms

Meta-heuristic techniques, which are mostly derivation-free, are iterative procedures for finding the best solutions in a parameter searching space. The techniques are preferred in non-convex or non-smooth problems where a mathematical relationship cannot be structured between the objective and the optimisation functions of the problem. One of the most popular processes in engineering applications that seek to simultaneously optimise various objective functions is the multi-objective optimisation problem. The multi-objective problems guarantee the acquisition of a complete set of optimal trade-offs, in contrast to single-objective optimisation problems. The popular bio-inspired meta-heuristics techniques are briefly described in this section, along with some of their advantages and disadvantages. The authors are responsible for obtaining any security clearances.

1. Multi-verse optimisation algorithm

The multi-verse optimisation algorithm was obtained by considering the different tasks of black holes, white holes, and wormholes in a universe. White holes and black holes are used to explore the search space. The wormhole tunnel and the white/black hole tunnel allow the best solutions to pass between the universes. The universes with white and black holes have different inflation rates. According to the inflation rates of the universes, white and black holes pass through the tunnels to the best universe. After creating the best universe, the best solution is chosen from this group. The weighting coefficients of the algorithm decrease exponentially with each iteration. In the case where second random variable is lower than the wormhole existence probability, the universe (U) is given as:

$$U_i^j = \begin{cases} U_i = u_b(m) + T\Delta(m) r_4 + lb(m),\ r_3 < 0{,}5, \\ U_i = u_b(m) - T\Delta(m) r_4 + lb(m),\ r_3 > 0{,}5, \end{cases} \quad (1)$$

$$T = 1 - \frac{l^{1/p}}{L^{1/p}}, \quad (2)$$

$$W = min + l\frac{max - min}{L}, \quad (3)$$

where m is the object number, u_b is the best universe created

so far, r_{1-4} is the random numbers in the range of [0, 1], T is the travel distance rate, W is the probability of existence of the wormhole, *ub* is the upper bound of the related iteration, L is the maximum iteration, l is the current iteration, $\Delta(m)$ is the difference between the upper and lower bounds, and *lb* is the lower bound of the iteration. The algorithm decides with multiple random values before reaching a conclusion. The global solutions of parameters in a very large search space are obtained without any deviations. The basic pseudo-code of the MVO algorithm is presented in Algorithm 1, where k is the number of universes created, *max* is the maximum numbers of the universes, and γ is the H∞ index of a control system from external inputs of the control system to any performance outputs.

Algorithm 1. Basic pseudo-code of the MVO algorithm.

Input: Initial controller coefficients
Output: Optimised controller and γ
Each universe denoted by the *k* number
Each object denoted by *m* number
for k = 1:*max*
  for m = 1: *max*
    r_2 = *random* [0, 1]
    if $r_2 < W$
      r_3 = *random* [0, 1], r_3 = *random* [0, 1]
      if $r_3 < W$
      $U_i^j = u_b(m) + T\Delta(m)r_4 + lb(m)$
      else
      $U_i^j = u_b(m) - T\Delta(m)r_4 + lb(m)$ **end**
    end
  end
end

2. Grey wolf optimisation algorithm

The grey wolf optimisation algorithm is an algorithm inspired by the hierarchical hunting strategy of grey wolves in nature. The wolves are divided into four different subsets, i.e., alpha, beta, delta, and omega wolves according to affinity order to prey. The alpha wolf represents the best solution, the beta wolf represents the second best solution, and the delta wolf represents the third best solution of the optimisation algorithm. The omega wolves represent the rest of the candidate solutions. The stages of the algorithm consist of three separate sub-steps, i.e., searching for prey, finding the prey, and attacking the prey parts.

Algorithm 2. Basic pseudo-code of the GWO algorithm.

Input: Initial controller coefficients
Output: Optimised controller and γ
Initialise all parameters
$\overrightarrow{X_{\alpha,\beta,\delta}}$ denotes the alpha, beta, and delta wolves populations
while i = 1: *max*
  for *each search agent*
    Update the current positions
  end
  Update related coefficients
  Calculate the objective functions of the all search agents
  Update the populations of alpha, beta, and delta wolves
  $i = i + 1$
end

After the wolves locate the prey, the arithmetic average of the current best three distance values is calculated to reach the optimal distance value for the next iteration of the algorithm. Since the location is updated in each iteration, a solution can be searched in a large searching space. The basic pseudo-code of the GWO algorithm is presented in Algorithm 2, where $\overrightarrow{X_i}$ is the position vectors of all wolves and i is the iteration number.

3. Whale optimisation algorithm

The whale optimisation algorithm is a method inspired by the hunting method of humpback whales. Unlike the previous algorithm, whales can approach their prey with two different trajectories for position updates of the whales. The first is a classical linear trajectory like the previous GWO algorithm, while the other is a spiral trajectory. In this way, the whales find the global solution with a minimum deviation of the prey in the wide search space. The coefficients, linear and spiral updating vectors of the whale positions are defined as:

$$\vec{A}_w = 2ar - a, \tag{4}$$

$$\vec{C}_w = 2r, \tag{5}$$

$$\vec{D}_w = \left|\vec{C}_w \vec{X}_w^* - \vec{X}_w(t)\right|, \tag{6}$$

$$\overrightarrow{X_w}(t+1) = \begin{cases} \left|\vec{X}_w^* - \vec{A}_w \vec{D}_w\right|, & p < 0.5, \\ \left|\vec{D}_w e^{bl}\cos(2\pi l) + \vec{X}_w^*(t)\right|, & p > 0.5, \end{cases} \tag{7}$$

where p is a random value in the range of [0, 1], $\vec{A}_w$ and $\vec{C}_w$ are the coefficient vectors, $\vec{X}_w^*$ is the whale position vector of the best solution, $\vec{D}_w$ is the displacement vector of the whales, l_w is the random number between [-1, 1], b is the user-defined constant for $\vec{r}$ is the random value in the logarithmic spiral shaping range and of [0, 1]. The vector a is a variable used to attack the prey stage. The basic pseudo-code of the WOA algorithm is given in Algorithm 3.

Algorithm 3. Basic pseudo-code of the WOA algorithm.

Input: Initial controller coefficients
Output: Optimised controller and γ
Initialise all parameters
while i = 1: *max*
  for *each search agent*
    if $p < 0.5$
      if $A < 1$
      Update the positions by solving (6)
      else
      Update the positions by solving (7)
      end
    else
    Update the positions by solving (7)
    end
  end
  Update related coefficients
  Calculate the objective functions of the all search agents
end

4. Multi-objective grey wolf optimisation algorithm

The multi-objective grey wolf optimisation algorithm is an extended version of the grey wolf algorithm to a multi-objective algorithm via combination with the Pareto front approach. The stages of searching for prey, hunting the prey,

and attacking the prey are the same as of the GWO algorithm. The resulting solutions are added to an archive. The best solution is selected by comparing the solutions in the archive. It has evolved into an effective multi-objective global algorithm using Pareto optimality and an archive part of the algorithm results. A leader selection mechanism, as well as a grid mechanism, are employed in the algorithm to update and trade non-dominated Pareto optimal solutions. For the searching stage of the algorithm, the main coefficients of the three wolves are defined as:

$$\vec{A}_n = 2ar_1 - a, \tag{8}$$

$$\vec{C}_n = 2r_2, \quad n = 1,2,3, \tag{9}$$

where *a* coefficient decreases linearly from 2 to 0, $\vec{A}_n$ and $\vec{C}_n$ denote the coefficients. For the hunting stage of the algorithm, the displacement vectors and impact vectors to position updates the three wolves are defined as:

$$\vec{D}_\alpha = \left|\vec{C}_1.\vec{X}_\alpha - \vec{X}\right|, \tag{10}$$

$$\vec{D}_\beta = \left|\vec{C}_1.\vec{X}_\beta - \vec{X}\right|, \tag{11}$$

$$\vec{D}_\delta = \left|\vec{C}_1.\vec{X}_\delta - \vec{X}\right|, \tag{12}$$

$$\vec{X}_1 = \left|\vec{X}_\alpha - \vec{A}_1\vec{D}_\alpha\right|, \tag{13}$$

$$\vec{X}_2 = \left|\vec{X}_\beta - \vec{A}_1\vec{D}_\beta\right|, \tag{14}$$

$$\vec{X}_3 = \left|\vec{X}_\delta - \vec{A}_1\vec{D}_\delta\right|, \tag{15}$$

where $\vec{D}$ denotes the displacement vector, $\vec{X}_\alpha$ is the position vector of the alpha wolf, $\vec{X}_\beta$ is the position vector of the beta wolf, $\vec{X}_\delta$ is the position vector of the delta wolf, and $\vec{X}$ denotes the position vector of the wolves. It must be linearly reduced at each iteration to obtain the global solution without any deviation. In the hunting step, the arithmetic mean of the best positions is calculated as

$$\vec{X}(t+1) = \frac{\vec{X}_1 + \vec{X}_2 + \vec{X}_3}{3}, \tag{16}$$

where $\vec{X}(t+1)$ is the position of the omega wolves used in the next iteration. The basic pseudo-code of the MOGWO algorithm is given in Algorithm 4.

Algorithm 4. Basic pseudo-code of the MOGWO algorithm.

Input: Initial controller coefficients
Output: Optimised controller and γ
Initialise all parameters
Find the non-dominated solutions, send them to the archive, and select best solution as alpha wolves
Find the second best solution from the archive as beta wolves
Find the third best solution from the archive as delta wolves
while *i* = 1: *max*
  for *each search agent*
    Update the current positions by solving (5), (6), (8), (9), (10), (11), (12), (13), (14), (15)
  end
  Update related coefficients
  Calculate the objective functions of the all search agents
  Update the archive according to the non-dominated solutions
  If the archive is full, then run the grid mechanism
  Restore alpha and beta to the archive
  i = i + 1
end

III. LOW-FREQUENCY MULTI-VARIABLE MODELS OF THE SYSTEM

The closed-loop power system of the IBC is presented in Fig. 1, where v_{in} is the source voltage, v_{Co} is the capacitor voltage, R is the load resistance, v_o is the output voltage of the converter, i_{l1} and i_{l2} are the inductance currents, i_{in} is the source current, V_{g1} and V_{g2} are the gate signals of the converter, and i_o is the load current. The converter includes two branch low-pass filters where inductances are denoted by $L_{1,2}$ with resistances denoted by r_L. The capacitance is denoted by C and is accompanied by a series resistance r_c. MOSFETs and diodes are denoted by $SW_{1,2}$ and $DIO_{1,2}$, respectively, with on resistances r_{mos} of the active ones. Mode I-IV represents the converter modes according to the on-off states of the active converter switches. Other components are used for closed-loop power converter control.

The control-to-output variable model of the converter is given in (17) with all possible parasitic resistances [35]

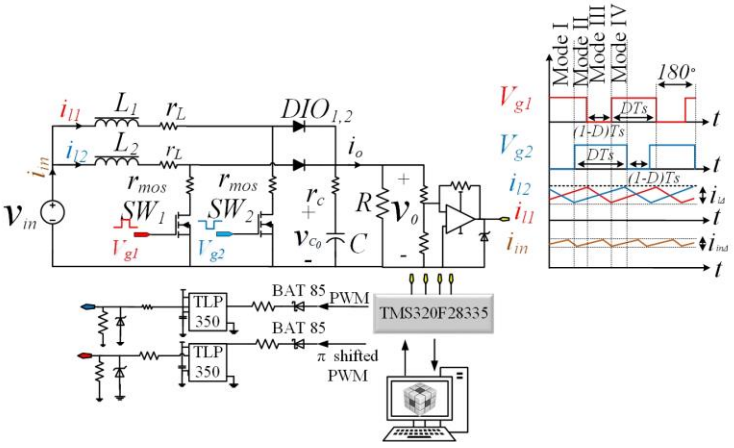

Fig. 1. Digital controlled closed-loop system of DC-DC.

$$G_{nom}(s)=\frac{(-V_o(Cr_cs+1)(R^2(4D-2D^2-2)+R(r_c+r_{mos})+r_c(r_L+r_{mos})+Ls(R+r_c))}{(D-1)(CLs^2(R^2+2Rr_c+r_c^2)+CDRs(r_{mos}-r_c)-r_c^2+2r_{mos}r_c)+CRs(R(r_c+r_L)+2r_cr_L+r_c^2)+LsR+Cr_c^2s(Dr_{mos}r_L)}. \quad (17)$$

The control input, external inputs of the robust H∞ control system, and performance outputs are presented in Fig. 2. Control-to-output transfer function is denoted by G_{nom}, and reference weighting is denoted by W_r, and noise weight is denoted by W_n. The error, control signal, and measured variable weighting functions are denoted by W_1, W_2, W_3, respectively. K is the feedback controller. The state-space representation of the open-loop control system presented in Fig. 2 can be given as

$$P=\begin{cases} Ax+B_{w1}w+B_{2u}u, \\ C_1x+D_{11w}w+D_{12u}u, \\ C_2x+D_{21w}w+D_{22u}u, \end{cases} \quad (18)$$

where $B_{1w}\subset R^{6x2}$ is the external input to state matrix, $B_{2u}\subset R^{6x1}$ is the duty cycle to state matrix, $D_{11w}\subset R^{3x2}$ is the external input to performance outputs matrix, $D_{12u}\subset R^{3x1}$ is the duty cycle to performance outputs matrix, $D_{21w}\subset R^{1x2}$ is the external input to output voltage of the converter without noise matrix, $D_{22u}\subset R^{1x1}$ is the duty cycle to performance outputs matrix. The main three sensitivity functions of the control system are obtained from Fig. 2 as follows:

$$S=\frac{1}{1+G_{nom}(s)K(s)}, \quad (19)$$

$$T=\frac{y_m}{n}=\frac{-G_{nom}(s)K(s)W_n(s)}{1+G_{nom}(s)K(s)}, \quad (20)$$

$$Q_{in}=\frac{u}{r}=\frac{K(s)}{1+G_{nom}(s)K(s)}. \quad (21)$$

Finally, the non-convex controller synthesis problem is structured as a mixed-sensitivity problem as

$$\begin{aligned} &\min_{K,\gamma} && \gamma \\ &st && \|W_1(s)S(s)\|_\infty\le\gamma, \\ & && \|W_3(s)T(s)\|_\infty\le\gamma, \\ & && \|W_2(s)Q_{in}(s)\|_\infty\le\gamma, \end{aligned} \quad (22)$$

where γ is an auxiliary variable that indicates the upper boundaries of the singular values of the sensitivity function. This scalar value is the main parameter that may determine the stability and performance of the system. However, it does not contain information on time-domain performance. The gamma value is heavily dependant on the performance weighting functions. These functions characterise the controller gain in the frequency area. The weighting functions are constructed as first-order transfer functions as:

$$W_1(s)=\frac{s/M_m+w_{be}}{s+w_{be}A_e}, \quad (23)$$

$$W_2(s)=\frac{s/M_u+w_{bu}}{s+w_{bu}A_u}, \quad (24)$$

$$W_3(s)=\frac{s/M_t+w_{bt}}{s+w_{bt}A_t}, \quad (25)$$

where w_{be}, w_{bu}, w_{bt} are the cut-off frequencies of the related weights, A_e, A_u, A_t are the low-frequency gain, and M_m, M_u, M_t are the high-frequency gains of the weighting functions. The weighting functions are optimised by selecting these nine variables. To optimise related functions, the proposed flowchart of the optimisation process is presented in Fig. 3. The design procedure of the approach consists of two steps: the first step is the inner loop, and the second step is the outer loop. In the inner loop, the control synthesis problem is solved using the two-Riccati approach and the calculated minimum objective function (γ) value. The full-order controller synthesis problem with two-Riccati equations is given by

$$\begin{aligned} &\min_{\psi} \gamma \\ &A^TX+XA+C_1^TC_1+X(\gamma^{-2}B_{1w}B_{1w}^T-B_{2u}B_{2u}^T)X=0, \\ &A^TY+AY+B_{1w}B_{1w}^T+Y(\gamma^{-2}C_1^TC_1-C_2^TC_2)Y=0, \\ &\rho(XY)<\gamma^2, \end{aligned} \quad (26)$$

where $\psi \triangleq \gamma$, X, Y. The robust controller K is given by

$$M_\infty=-B_{2u}^TX, \quad (27)$$

$$R_\infty=-YC_2^T, \quad (28)$$

$$T_\infty=(I-\gamma^{-2}YX)^{-1}, \quad (29)$$

$$N_\infty=A-\gamma^{-2}B_{1w}B_{1w}^TXB_{2u}M_\infty+T_\infty R_\infty C_2, \quad (30)$$

$$K=\begin{bmatrix} N_\infty & -T_\infty R_\infty & T_\infty B_{2u} \\ M_\infty & 0 & I \\ -C_2 & I & 0 \end{bmatrix}, \quad (31)$$

where X and Y are the real positive matrices and ρ is the magnitude of the eigenvalues. In the outer loop, the related parameters of the weighting functions are optimised with the single-objective and proposed multi-objective algorithm. To reflect the dynamic characteristics and robustness issues of the control system, the proposed objective function (J_1 and J_2) involves incremental squared error (ISE) of the converter output voltage as the measured variable and infinite norm of the metrics of the closed-loop control system. The infinite norm index function and the ISE can be expressed as:

$$J_1=\int_0^t e^2dt, \quad (32)$$

$$J_2=\gamma=\sup\bar{\sigma}\begin{bmatrix} W_1(iw)S(iw) \\ W_2(iw)Q_{in}(iw) \\ W_3(iw)T(iw) \end{bmatrix}, \quad (33)$$

where t is the tolerance value for time, w is the radian frequency, and $\bar{\sigma}$ is the maximum singular value of a matrix. In addition, the converter is a non-minimum phase system. The weighting function parameters should be limited for the stability of the systems. The main constraints of the optimisation problem are as follows. Constraint 1: The maximum closed-loop bandwidth must be less than the right half-plane zero frequency of the converter. Therefore, the frequency of the error weight W_1 given in (23) should be limited. Constraint 2: The infinity norm of the complementary sensitivity function should be between 1 dB and 5 dB. Constraint 3: The modulus margin (M_m) variable of the sensitivity weighting function must be less than the 1.5 amplitude value. This constraint ensures that the loop gain stays away from the instability point (-1) of the Nyquist graph [36]. Therefore, the stability of the system against parameter uncertainties of the converter is increased according to the Nyquist plot analysis. By minimising these objective functions, a controller is obtained that guarantees stability and performance. In the study, two different objective functions given in (32) and (33) are used in the proposed multi-objective control approach. The single-objective function that includes the gamma is utilised in the other algorithms. As a result of this choice, the gamma value may take a lower value for the GWO, MVO, and WOA algorithms-based approaches than the proposed multi-objective approach.

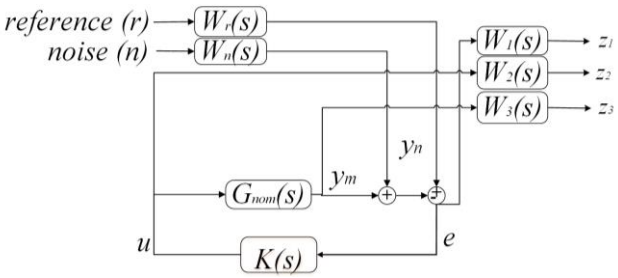

Fig. 2. The H∞ closed-loop control for noise suppression.

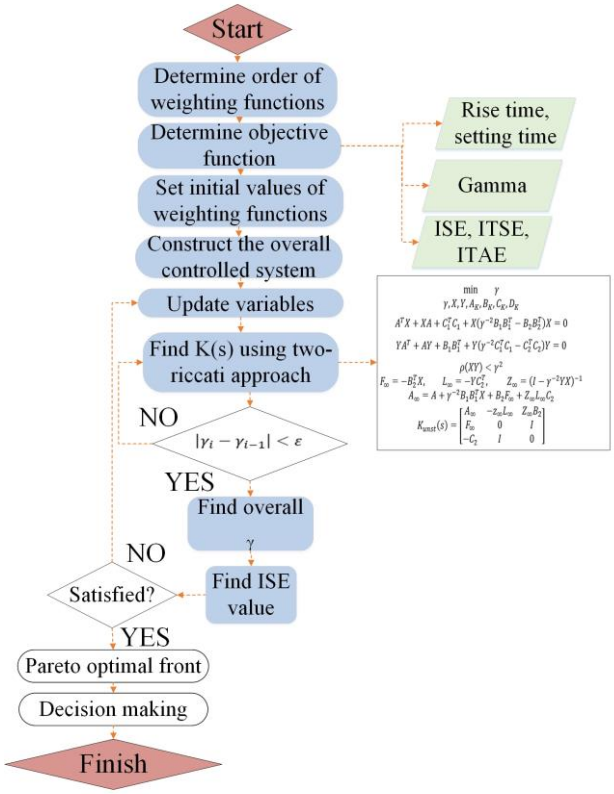

Fig. 3. Proposed flow-chart of the H∞ weighting optimisation technique.

IV. Simulation Results of the Optimised Closed-Loop Systems

The proposed approach which is based on H∞ and metaheuristic techniques is now applied to the specific disturbance situations of the closed-loop converter system. The purpose is to validate and compare the effectiveness of this design with single-objective meta-heuristic solutions. The upper and lower bounds of the optimisation parameters are selected for performance requirements as: i) worst-case overshoots: 18 %, ii) settling time: 100 ms, iii) steady-state error: 0.01 %, and iv) strong disturbance rejection ability. The optimisation problem computations are solved using Matlab 2019a software. The circuit parameters of the DC-DC power converter are given in Table I. The optimised and noise weighting functions using the proposed multi-

objective approach are given as:

$$W_1(s)=\frac{s+395}{1.4s+3.95\times10^{-7}}, \tag{34}$$

$$W_2(s)=\frac{s+1850}{0.04s+18500}, \tag{35}$$

$$W_3(s)=\frac{s+400}{15s+2000}, \tag{36}$$

$$W_n(s)=\frac{s+1481}{2s+148120}, \tag{37}$$

The variations of the objective functions are presented in Fig. 4. In the single-objective approaches, the MVO algorithm-based approach has a minimum gamma value over six iterations. In the proposed multi-objective algorithm, the minimisation of the gamma and the minimisation of the ISE function are aimed at obtaining disturbance rejection ability. In the proposed approach, the best ISE value taken from the archive is 1.65 and the gamma value is 0.732. In Fig. 4(b), it is seen that the optimum point for the MOGWO algorithm-based approach is selected from the two-axis frame. The gamma value cannot be considered the only performance criterion for performance comparison of the controllers achieved by using optimisation algorithms presented above. Therefore, the performance comparison is made over the time-domain performances. The optimal-robust controller gains using the proposed single- or multi-objective approaches are obtained as:

$$K_{mvo}=\frac{s^5+6\times10^8s^4+2\times10^{14}s^3+6\times10^{18}s^2+10^{21}s+5\times10^{23}}{s^6+5\times10^5s^5+5\times10^4s^4+2\times10^3s^3+10^{19}s^2+10^{23}s^1+2\times10^{19}}, \tag{38}$$

$$K_{gwo}=\frac{4\times10^6s^5+9\times10^{11}s^4+3\times10^{16}s^3+10^{20}s^2+10^{22}s+10^{25}}{s^6+3\times10^8s^5+3\times10^{13}s^4+3\times10^7s^3+10^{21}s^2+10^{24}s^1+8\times10^{22}}, \tag{39}$$

$$K_{woa}=\frac{s^5+3\times10^{11}s^4+4\times10^3s^3+9\times10^{20}s^2+2\times10^{23}s+8\times10^{25}}{s^6+4\times10^5s^5+5\times10^4s^4+3\times10^{17}s^3+10^{21}s^2+10^{25}s^1+10^{22}}, \tag{40}$$

$$K_{mogwo}=\frac{10^6s^5+5\times10^{11}s^4+5\times10^{16}s^3+10^{21}s^2+2\times10^{23}s+9\times10^{25}}{s^6+10^7s^5+7\times10^{12}s^4+23\times10^{17}s^3+10^{21}s^2+10^{25}s^1+1\times10^{22}}, \tag{41}$$

where the order of the controllers is equal to total order of the nominal model and the weighting functions. We now present time-domain performances from a simulation study of the converter. The control design is created using the Matlab/Simulink programme and is based on the electrical network of the equivalent prototype shown in Fig. 1 in order to investigate the performance of the proposed approach.

The output voltages of the controlled systems are presented in Fig. 5(a). Variations in the input voltage and load current of the converter are presented in Fig. 5(b) and Fig. 5(c). At the start of the converter, the input voltage is 46 V and the load resistance is 20 Ω.

By comparing the output voltage responses, it can be seen that the controlled systems are enabled to have some overshoots lower than predefined 18 % at the starting process. The K_{mogwo} controlled system has minimum overshoots at disturbance moments as presented in Fig. 5. The controllers have nearly 9 %−16 % overshoots at the starting of the converter. These values are acceptable, since the main purpose of the application is to reject disturbances and uncertainties. The set-point signal is changed to a 90 V value at t = 0.3 s and then increased to a nominal value to test the set-point tracking performance of the systems. Input voltage and load current disturbances are changed in simulation studies to test the disturbance rejection ability of the controlled systems. First, the input voltage is increased to 58 V (+16 % of the nominal value) at t = 1 s and 4 s. It is decreased by 16 % of the nominal value at t = 1.5, 3.5, and 4.3 seconds. The load resistance is changed stepwise from R = 20 Ω to R = 200 Ω at t = 2 s, from R = 200 Ω to R = 250 Ω at t = 2.5 s, and from R = 250 Ω to R = 300 Ω at t = 3 s. Controlled systems prevent oscillations on the output voltage of the converter. These supreme performances are achieved by providing the phase margin of open-loop gains closer to 80 degrees. The controllers optimised by the single-objective approaches are able to reject the disturbances; however, the K_{mogwo} controller has supreme disturbance rejection capability in the presence of all parameter variations.

TABLE I. CIRCUIT PARAMETERS OF THE POWER CIRCUIT.

Parameter	Nominal Value
R	50 Ω
C	0.98 mF
L_1=L_2	5.07 mH
r_L	0.582 Ω
r_c	0.1 Ω
r_{mos}	0.036 Ω
v_{in}	46 V
v_o	100 V
f	10 kHz

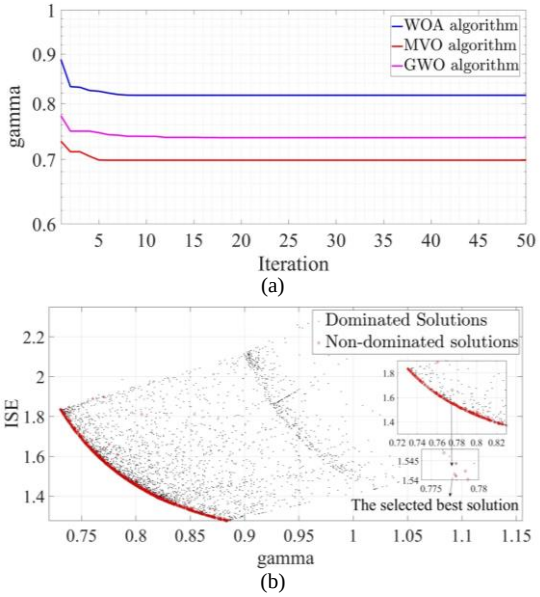

Fig. 4. Variations of objective functions: (a) Single-objective optimisation results; (b) The proposed multi-objective results.

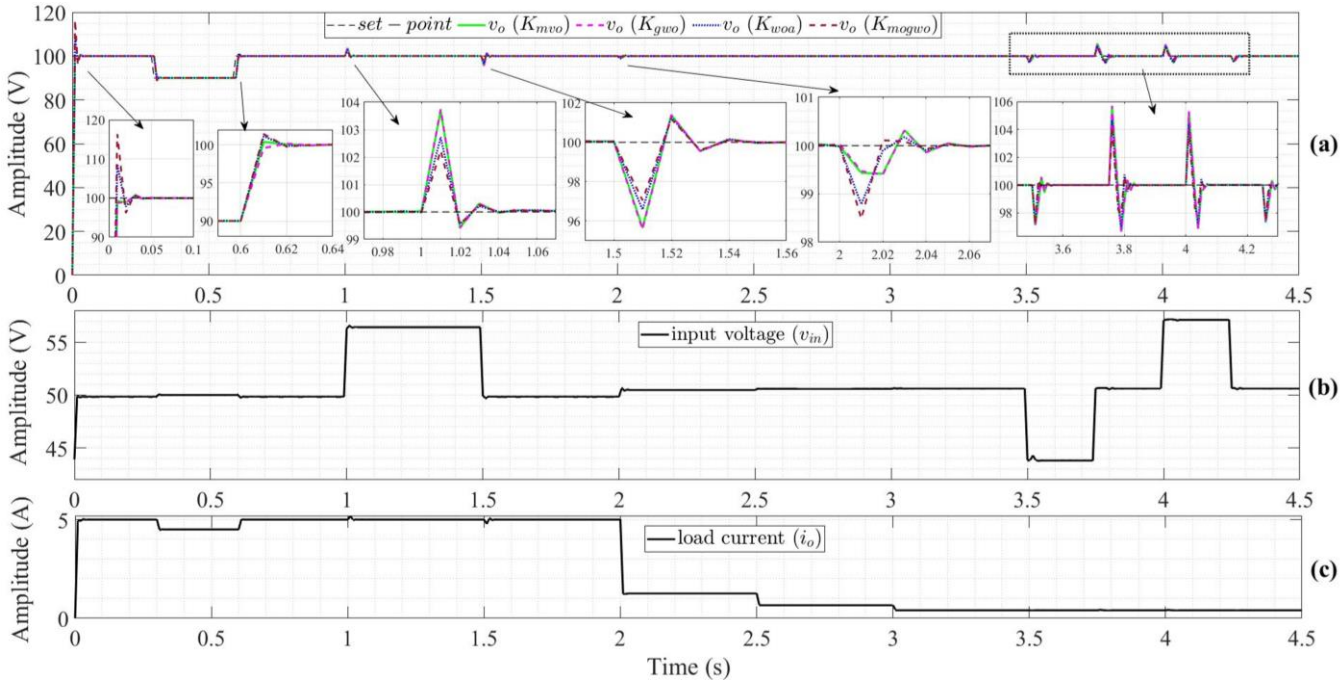

Fig. 5. Results of the time-domain performance of the controlled closed-loop systems: (a) Output voltage; (b) Input voltage variations; (c) Load current variations of the converter.

V. EXPERIMENTAL RESULTS

A digital signal processor (DSP)-based real-time implementation results of the closed-loop converter are presented to verify the practical performance of the approach. A Texas Instrument TMS320F28335 processor is used to implement controllers and data recording. A Sorensen programmable DC source and an adjustable resistor (0 kΩ−1 kΩ) are used to implement disturbance effects on the converter. The hardware-in-the-loop system of the experimental prototype is presented in Fig. 6. At the starting, set-point tracking, and disturbance rejection performances of the optimised controller using the MVO algorithm-based approach are presented in Fig. 7.

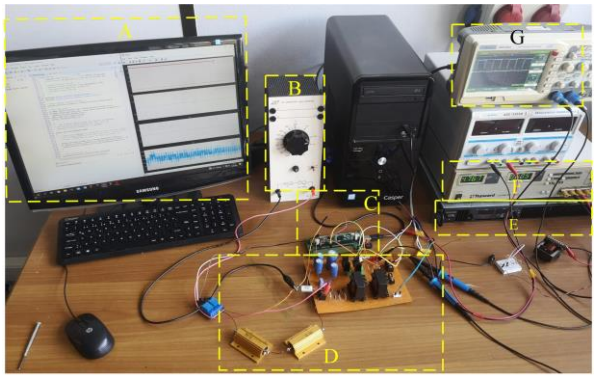

Fig. 6. Hardware-in-the-loop test system of the power converter: (A) Host computer; (B) 300 W adjustable resistance; (C) TMS320F28335 digital processor; (D) 200 W two-phase interleaved boost converter circuit; (E) Sorensen 1500 W programmable DC power supply; (F) Topward LCR meter; (G) AA-TECH digital oscilloscope to monitor gate signals of the converter.

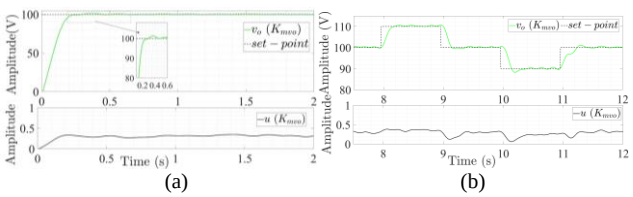

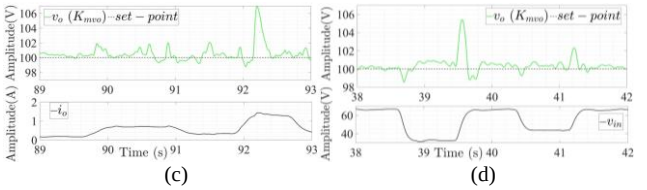

Fig. 7. Real-time application results of the MVO optimised: (a) Point 1: Starting of the converter; (b) Point 2: Set-point changes; (c) Point 3: Load changes; (d) Point 4: Input voltage changes.

In point 1, the K_{mvo} controlled system has 1.4 % overshoot at starting and 290 ms settling-time. The set-point tracking performance of the controller can be seen in Fig. 7(b). At point 3, the controller has 6.9 V overshoot during load current changes at the 92nd second of Fig. 7(c). In point 4, the controller has 5.4 V overshoot during input voltage changes at 39.45th second of Fig. 7(d). The controller has the ability to reject disturbances and minimise overshoots at set-point changes. At starting, set-point tracking and disturbance rejection performances of the optimised controller using the GWO algorithm-based approach are presented in Fig. 8. In point 5, the K_{gwo} controlled system has 2 % overshoot at starting and 310 ms settling time. The set-point tracking performance of the controlled system can be seen in Fig. 8(b). In point 7, the controller has 3.5 V overshoot during load current changes at 80.88th second of Fig. 8(c). In point 8, the controlled system has 1.7 V overshoot during input voltage changes at 56.79th second of Fig. 8(d). The controlled system has the ability to reject disturbances and have minimal overshoots at set-point changes. These performance findings are similar to the performance of the K_{mvo} controlled system. The time-domain performances of the controlled systems are also very similar in the simulation study. The controllers have similar tracking and disturbance rejection performance. 5 % overshoot and oscillation differences between the signals are caused by noise. At the starting, set-point tracking and disturbance rejection performances of the optimised

controller using the WOA algorithm-based approach (blue line) are presented in Fig. 9.

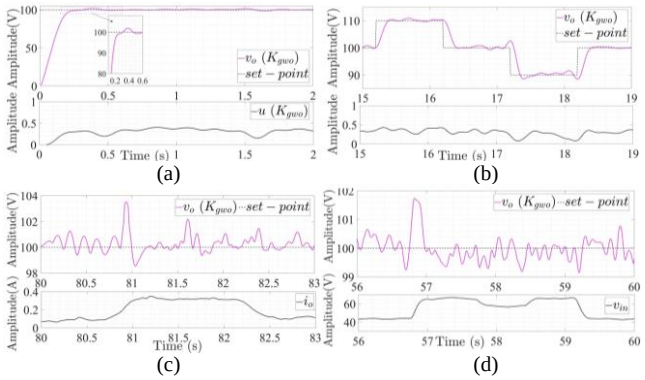

Fig. 8. Real-time application results of the GWO optimised: (a) Point 1: Starting of the converter; (b) Point 2: Set-point changes; (c) Point 3: Load changes; (d) Point 4: Input voltage changes.

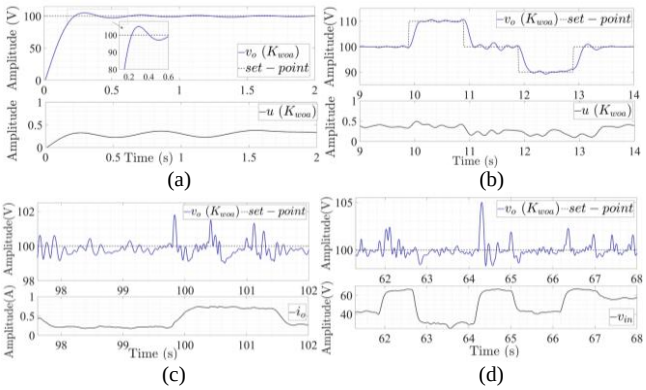

Fig. 9. Real-time application results of the WOA optimised: (a) Point 1: Starting of the converter; (b) Point 2: Set-point changes; (c) Point 3: Load changes; (d) Point 4: Input voltage changes.

In point 9, the K_{woa} controlled closed-loop system has a 4.95 % overshoot at starting and 400 ms settling time. The set-point tracking performance of the system can be seen in Fig. 9(b). In point 11, the controlled system has 1.8 V overshoot during load current changes at 99.4th second of Fig. 9(c). In point 12, the controlled system has 5 V overshoot during input voltage changes at 64.4th second of Fig. 9(d). The controlled system has a better ability to reject disturbances than previous closed-loop systems. However, it has overshoots and oscillations at the parameter variations of the converter.

Figure 10 demonstrates the set-point tracking and disturbance rejection performance of the optimised controller using the proposed MOGWO algorithm-based approach. At the starting of the controlled system, the controlled system has 12.5 % overshoot and 680 ms settling time. The set-point tracking performance of the system can be seen in Fig. 10(b). Figure 10(c) demonstrates the rejection performances of the load disturbance effects caused by varying the load current around high- and low-power working conditions on the output voltage. The load resistance is changed stepwise from R = 532 Ω to R = 156 Ω at t = 67.2 s, from R = 156 Ω to R = 322.6 Ω at t = 68.1 s, and from R = 322.6 Ω to R = 73 Ω at t = 69 s. The proposed controlled system has slight oscillations under load current variations due to boosting the phase margin of the controlled system to the requested levels. In point 16, the system has 3.04 V overshoot during input voltage changes at 50.56th second of Fig. 10(d). As previously in the experimental performance analysis, the disturbance rejection performance of the K_{mogwo} controlled closed-loop system still has the lowest overshoots under input voltage and load current changes. The controller has the best disturbance rejection ability of the other optimised controllers. However, it has overshoots and oscillations at the starting of the converter. The increase in disturbance rejection performance resulted in a decrease in performance at the reference changes. However, this can be ignored since the main purpose of the circuit is to keep the output voltage constant under disturbance conditions. The slight differences between the simulation and experiment results in Fig. 10 are due to minor differences in the input voltage and load current variations. It is important to note that such a disconformity is due to the difference in sensitivity of the programmable power supplies in simulation and experiments and the inevitable errors implied in practise by the measuring sensors. Also, heating of the passive components or sensor noise can cause such minor mismatches.

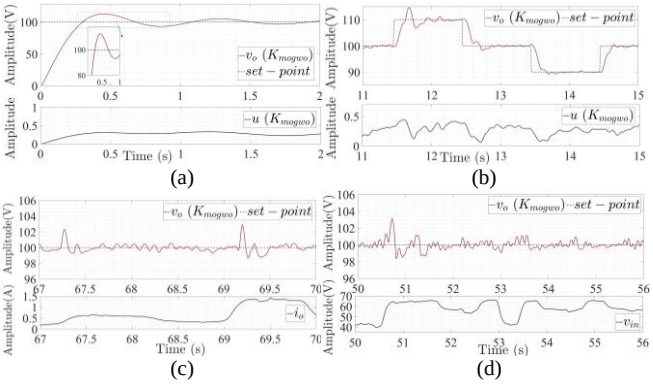

Fig. 10. Real-time application results of the MOGWO optimised: (a) Point 1: Starting of the converter; (b) Point 2: Set-point changes; (c) Point 3: Load changes; (d) Point 4: Input voltage changes.

VI. RESULTS AND DISCUSSION

A robust H∞ control theory and the multi-objective algorithm-based full-order controller synthesis approach is proposed to regulate the output voltage of the interleaved boost converter under severe disturbances. The automated design of closed-loop systems is enabled by the synthesis of a robust controller with optimisation of the performance weighting functions using the proposed multi-objective and single-objective meta-heuristic algorithms. The proposed flowchart of the controller synthesis process is utilised for robustness and transient response performances with maximum overshoot, settling time, step change error, and infinite norm ‖.‖∞ metrics. Thanks to this weighting design approach, which utilises multi-objective optimisation, the disturbance rejection performance of the closed-loop control system is increased. The proposed multi-objective design approach is tested and compared to algorithms such as the MVO, GWO, and WOA optimisation algorithms which utilise the single-objective cost function. The simulation and experimental results demonstrate that all of the approaches successfully eliminate the steady-state error of the output voltage. Although the variation of the input voltage is significant (±44 %) in the experimental setup, the output voltage has a small deviation of a maximum of 240 ms and returns to the nominal set-point value without oscillations.

The load current is changed between +150 % and -85 % of the nominal value in the simulation study. In the experimental setup, the load current is changed between -30 % and -95 % of the nominal value. The output voltage presents small overshoots less than 2.9 % of the nominal value during the load variations. The controller optimised with the proposed MOGWO algorithm-based robust control approach significantly suppresses the influenced of the input voltage and load current disturbances.

CONFLICTS OF INTEREST

The authors declare that they have no conflicts of interest.

REFERENCES

[1] D. Ghaderi, M. Celebi, M. R. Minaz, and M. Toren, "Efficiency improvement for a DC-DC quadratic power boost converter by applying a switch turn-off lossless snubber structure based on zero voltage switching", *Elektronika ir Elektrotechnika*, vol. 24, no. 3, pp. 15–22, 2018. DOI: 10.5755/j01.eie.24.3.20977.

[2] M. A. Vaghela and M. A. Mulla, "Ultra-high step-up gain interleaved coupled inductor DC–DC converter with reduced voltage stress and eliminated right half plane zero", *Arabian Journal for Science and Engineering*, pp. 1–20, 2022. DOI: 10.1007/s13369-022-07375-3.

[3] A. Rahimi, V. Ranjbarizad, and E. Babaei, "Interleaved buck–boost n-phase high-efficiency converter with soft switching and low output voltage ripple", *Arabian Journal for Science and Engineering*, vol. 46, pp. 9497–9513, 2021. DOI: 10.1007/s13369-021-05337-9.

[4] C.-S. Chiu and S. Ngo, "A novel algorithm-based MPPT strategy for PV power systems under partial shading conditions", *Elektronika ir Elektrotechnika*, vol. 28, no. 1, pp. 42–51, 2022. DOI: 10.5755/j02.eie.30183.

[5] H. Armghan, I. Ahmad, N. Ali, M. F. Munir, S. Khan, and A. Armghan, "Nonlinear controller analysis of fuel cell–battery–ultracapacitor-based hybrid energy storage systems in electric vehicles", *Arabian Journal for Science and Engineering*, vol. 43, pp. 3123–3133, 2018. DOI: 10.1007/s13369-018-3137-y.

[6] P.-C. Chen, S.-M. Pan, H.-S. Chuang, and C.-H. Chiang, "Dynamics analysis and robust control for electric unicycles under constrained control force", *Arabian Journal for Science and Engineering*, vol. 41, pp. 4487–4507, 2016. DOI: 10.1007/s13369-016-2163-x.

[7] I. Aharon, D. Shmilovitz, and A. Kuperman, "Robust output voltage control of multimode non-inverting DC–DC converter", *International Journal of Control*, vol. 90, no. 1, pp. 110–120, 2017. DOI: 10.1080/00207179.2015.1122839.

[8] J. Karlsson, T. T. Georgiou, and A. G. Lindquist, "The inverse problem of analytic interpolation with degree constraint and weight selection for control synthesis", *IEEE Trans. on Automatic Control*, vol. 55, no. 2, pp. 405–418, 2010. DOI: 10.1109/TAC.2009.2037280.

[9] S. M. Raafat, R. Akmeliawati, and I. Abdulljabaar, "Robust H_∞ controller for high precision positioning system, design, analysis, and implementation", *Intelligent Control and Automation*, vol. 3, no. 3, 2012. DOI: 10.4236/ica.2012.33030.

[10] M. Dulau and S.-E. Oltean, "The effects of weighting functions on the performances of robust control systems", *Proceedings*, vol. 63, no. 1, p. 46, 2020. DOI: 10.3390/proceedings2020063046.

[11] R. Sanchis and I. Penarrocha, "A PID tuning approach to find the optimal˜ compromise among robustness, performance and control effort: implementation in a free software tool", *International Journal of Control*, pp. 1–20, 2021. DOI: 10.1080/00207179.2021.1989491.

[12] J. Hu, C. Bohn, and H. Wu, "Systematic H_∞ weighting function selection and its application to the real-time control of a vertical take-off aircraft", *Control Engineering Practice*, vol. 8, no. 3, pp. 241–252, 2000. DOI: 10.1016/S0967-0661(99)00157-4.

[13] S. P. Diwan and S. S. Deshpande, "Fast nonlinear model predictive controller using parallel PSO based on divide and conquer approach", *International Journal of Control*, just-accepted, 2022. DOI: 10.1080/00207179.2022.2087739.

[14] S. Jaypuria, A. K. Das, P. K. C. Kanigalpula, D. Das, D. K. Pratihar, D. Chakrabarti, and M. N. Jha, "Swarm intelligence-based modeling and multi-objective optimization of welding defect in electron beam welding", *Arabian Journal for Science and Engineering*, vol. 48, pp. 1807–1827, 2023. DOI: 10.1007/s13369-022-07017-8.

[15] D. Whitley, "A genetic algorithm tutorial", *Statistics and Computing*, vol. 4, pp. 65–85, 1994. DOI: 10.1007/BF00175354.

[16] J. Wang and J. Yu, "Particle swarm optimization-based H∞ tracking fault tolerant control for batch processes", *IEEE Access*, vol. 9, pp. 84241–84251, 2021. DOI: 10.1109/ACCESS.2021.3087939.

[17] S. Unsal and I. Aliskan, "Investigation of performance of fuzzy logic controllers optimized with the hybrid genetic-gravitational search algorithm for PMSM speed control", *Automatika*, vol. 63, no. 2, pp. 313–327, 2022. DOI: 10.1080/00051144.2022.2036936.

[18] S. Mirjalili, S. M. Mirjalili, and A. Lewis, "Grey wolf optimizer", *Advances in Engineering Software*, vol. 69, pp. 46–61, 2014. DOI: 10.1016/j.advengsoft.2013.12.007.

[19] S. Mirjalili and A. Lewis, "The whale optimization algorithm", *Advances in Engineering Software*, vol. 95, pp. 51–67, 2016. DOI: 10.1016/j.advengsoft.2016.01.008.

[20] G. I. Sayed, A. Darwish, and A. E. Hassanien, "Quantum multiverse optimization algorithm for optimization problems", *Neural Computing and Applications*, vol. 31, pp. 2763–2780, 2019. DOI: 10.1007/s00521-017-3228-9.

[21] G. Eappen and T. Shankar, "Multi-objective modified grey wolf optimization algorithm for efficient spectrum sensing in the cognitive radio network", *Arabian Journal for Science and Engineering*, vol. 46, pp. 3115–3145, 2021. DOI: 10.1007/s13369-020-05084-3.

[22] H. Maghfiroh, M. Nizam, M. Anwar, and A. Ma'Arif, "Improved LQR control using PSO optimization and Kalman filter estimator", *IEEE Access*, vol. 10, pp. 18330–18337, 2022. DOI: 10.1109/ACCESS.2022.3149951.

[23] M. K. Habib and S. A. Ayankoso, "Hybrid control of a double linear inverted pendulum using LQR-fuzzy and LQR-PID controllers", in 2022 *IEEE International Conference on Mechatronics and Automation (ICMA)*, 2022, pp. 1784–1789. DOI: 10.1109/ICMA54519.2022.9856235.

[24] C. Kang, S. Wang, W. Ren, Y. Lu, and B. Wang, "Optimization design and application of active disturbance rejection controller based on intelligent algorithm", *IEEE Access*, vol. 7, pp. 59862–59870, 2019. DOI: 10.1109/ACCESS.2019.2909087.

[25] X.-K. Dang, V.-D. Do, and X.-P. Nguyen, "Robust adaptive fuzzy control using genetic algorithm for dynamic positioning system", *IEEE Access*, vol. 8, pp. 222077–222092, 2020. DOI: 10.1109/ACCESS.2020.3043453.

[26] J. Zietkiewicz, P. Kozierski, and W. Giernacki, "Particle swarm optimisation in nonlinear model predictive control; comprehensive simulation study for two selected problems", *International Journal of Control*, vol. 94, no. 10, pp. 2623–2639, 2021. DOI: 10.1080/00207179.2020.1727957.

[27] M. Ejaz and M. N. Arbab, "Automatic weight selection in H_∞ loop shaping using genetic algorithm", in *Proc. of 2006 International Conference on Emerging Technologies*, 2006, pp. 334–342. DOI: 10.1109/ICET.2006.335971.

[28] E. Alfaro-Cid, E. W. McGookin, and D. J. Murray-Smith, "Optimisation of the weighting functions of an H_∞ controller using genetic algorithms and structured genetic algorithms", *International Journal of Systems Science*, vol. 39, no. 4, pp. 335–347, 2008. DOI: 10.1080/00207720701777959.

[29] J. Dais and J. Yings, "Multivariable robust H∞ control for aeroengines using modified particle swarm optimization algorithm", in *Proc. of 2012 12th International Conference on Control Automation Robotics & Vision (ICARCV)*, 2012, pp. 1605–1609. DOI: 10.1109/ICARCV.2012.6485426.

[30] Y. Zou *et al.*, "Optimized robust controller design based on CPSOGSA optimization algorithm and H_2/H_∞ weights distribution method for load frequency control of micro-grid", *IEEE Access*, vol. 9, pp. 162093–162107, 2021. DOI: 10.1109/ACCESS.2021.3132729.

[31] E. Jiaqiang, C. Qian, H. Liu, and G. Liu, "Design of the H_∞ robust control for the piezoelectric actuator based on chaos optimization algorithm", *Aerospace Science and Technology*, vol. 47, pp. 238–246, 2015. DOI: 10.1016/j.ast.2015.09.026.

[32] S. Santra and S. Paul, "PSO based weight selection & static H∞ loop shaping controller design for robust power system stabilizer in four-block framework using LMI approach", in *Proc. of 2017 IEEE Calcutta Conference (CALCON)*, 2017, pp. 109–113. DOI: 10.1109/CALCON.2017.8280706.

[33] H. Wang, Y. Guo, G. Li, J. Lu, and X. Qi, "Aero-engine robust H(infinity) loop-shaping controller design based on genetic algorithm", in *Proc. of 2008 Second International Symposium on Intelligent Information Technology Application*, 2008, pp. 1035–1039. DOI: 10.1109/IITA.2008.253.

[34] S. Y. Zhang, C. B. Wei, J. Li, and J. H. Wu, "Robust H∞ controller based on multi objective genetic algorithms for active magnetic bearing applied to cryogenic centrifugal compressor", in *Proc. of 2017 29th Chinese Control And Decision Conference (CCDC)*, 2017, pp. 46–51. DOI: 10.1109/CCDC.2017.7978064.

[35] R. Keskin, I. Aliskan, and E. Das, "Robust structured controller synthesis for interleaved boost converters using an H_∞ control method", *Trans. of the Institute of Measurement and Control*, vol. 43, no. 14, pp. 3169–3180, 2021. DOI: 10.1177/01423312211019560.

[36] S. Skogestad and I. Postlethwaite, *Multivariable Feedback Control*: *Analysis and Design*. Wiley, 2005.